Available online at www.sciencedirect.com
SCIENCE DIRECT®
Thermochimica Acta 417 (2004) 67–73
thermochimica acta
www.elsevier.com/locate/tca

Two-state irreversible thermal denaturation of anionic peanut (*Arachis hypogaea* L.) peroxidase

Laura S. Zamorano [a], David G. Pina [b], Francisco Gavilanes [c], Manuel G. Roig [a], Ivan Yu. Sakharov [d], Andrei P. Jadan [e], Robert B. van Huystee [f], Enrique Villar [b], Valery L. Shnyrov [b,*]

[a] *Departamento de Química Física, Facultad de Química, Universidad de Salamanca, 37008 Salamanca, Spain*
[b] *Departamento de Bioquímica y Biología Molecular, Universidad de Salamanca, 37007 Salamanca, Spain*
[c] *Departamento de Bioquímica y Biología Molecular, Facultad de Química, Universidad Complutense, 28040 Madrid, Spain*
[d] *Department of Chemical Enzymology, Faculty of Chemistry, Moscow State University, 118899 Moscow, Russia*
[e] *Institute for Biological Instrumentation of the Russian Academy of Sciences, 142290 Pushchino, Moscow Region, Russia*
[f] *Department of Plant Sciences, The University of Western Ontario, London, Ont., Canada N6A 5B7*

Received 20 August 2003; received in revised form 19 January 2004; accepted 19 January 2004

Available online 5 March 2004

Abstract

Detailed differential scanning calorimetry (DSC), steady-state tryptophan fluorescence and far-UV circular dichroism (CD) studies, together with enzymatic assays, were carried out to monitor the thermal stability of anionic peanut peroxidase (aPrx) at pH 3.0. The spectral parameters were seen to be good complements to the highly sensitive but integral method of DSC. Thus, changes in far-UV CD corresponded to changes in the overall secondary structure of the enzyme, while changes in intrinsic tryptophan fluorescence emission corresponded to changes in the tertiary structure of the enzyme. The results, supported with data concerning changes in enzymatic activity with temperature, show that thermally induced transitions for aPrx are irreversible and strongly dependent upon the scan rate, suggesting that denaturation is under kinetic control. It is shown that the process of aPrx denaturation can be interpreted with sufficient accuracy in terms of the simple kinetic scheme, $N \xrightarrow{k} D$, where k is a first-order kinetic constant that changes with temperature, as given by the Arrhenius equation; N is the native state, and D is the denatured state. On the basis of this model, the parameters of the Arrhenius equation were calculated.

Keywords: Irreversible thermal denaturation; Differential scanning calorimetry; Intrinsic fluorescence; Circular dichroism; Peanut peroxidase

1. Introduction

Peroxidases are wide spread in plants, microbes, and animal tissues and represent a huge family of heme-containing proteins (see [1] and references therein). They are enzymes catalysing the oxidation of numerous organic and inorganic compounds by hydrogen peroxide or its derivatives. The heme peroxidase superfamily has been classified into three groups on the basis of amino acid sequence homology and metal-ion binding capabilities [2,3]. Class I comprises intracellular peroxidases, including cytochrome *c* peroxidase, ascorbate peroxidase and the gene-duplicated bacterial catalase-peroxidases. Class II contains the secretory fungal enzymes, such as manganese peroxidase and lignin peroxidase. Finally, class III, which includes aPrx, consists of the secretory plant peroxidases.

Peroxidases are important for various biotechnological purposes [4–6]. This group of enzymes, in particular those from plants, enjoys widespread use as catalysts for phenolic resin synthesis, as indicators for food processing and diagnostic reagents and as additives in bioremediation. Under specific conditions the radicals formed can break bonds in polymeric materials resulting in their destruction, for instance, in lignin biodegradation. An important peroxidase application is in production of conducting polymers such as polyaniline. Synthesis of polyaniline can occur in the presence of peroxidase, hydrogen peroxide as a reducing substrate, and sulfonated polystyrene and

* Corresponding author. Tel.: +34-923-294465; fax: +34-923-294579.
E-mail address: shnyrov@usal.es (V.L. Shnyrov).

0040-6031/$ – see front matter © 2004 Elsevier B.V. All rights reserved.
doi:10.1016/j.tca.2004.01.018

poly(vinyl-phosphonic acid) as polymeric templates at acidic pH values [7]. Consequently, for the development of such biotechnological processes, it is of interest to find and characterise peroxidases that are stable under acidic conditions.

Peanut peroxidase secreted in cell suspension medium, is a heme and calcium containing glyco-protein. Cationic peanut peroxidase (cPrx) shares 50% sequence homology with horseradish peroxidase (HRP) and structure of cPrx was the first determined for any class III peroxidase (see [8] and references therein). Secondary structure contents and key distal residues are conserved with the same numbering between HRP and cPrx. cPrx has three N-linked glycans accounting for 15–20% of its 40 kDa molecular weight [9]. But little is known about its anionic counterpart (aPrx) in spite of demonstration that cationic and anionic peroxidases, the two major peroxidases isolated from peanut cell culture, are similar in their physico-chemical, catalytic and immunological properties [10–12].

The present study describes the thermal stability of anionic (pI = 4.3) peanut (*Arachis hypegaea*, Leguminosae) peroxidase (EC 1.11.1.7) at pH 3.0. This was investigated by differential scanning calorimetry (DSC) in combination with intrinsic fluorescence and circular dichroism (CD) as well as enzymatic activity assays. Thermal denaturation of aPrx was found to be irreversible and strongly scan-rate dependent, which led us to analyse the reaction based on the simplest two-state kinetic model:

$$\mathrm{N} \xrightarrow{k} \mathrm{D} \quad (1)$$

which is a limiting case of the Lumry–Eyring model [13]. This model considers only two significantly populated macroscopic states, the initial or native state (N) and the final or denatured state (D), transition between which is determined by a strongly temperature-dependent first-order rate constant (k).

2. Experimental

Guaiacol (2-methoxyphenol) was purchased from Sigma (St. Louis, MO, USA). H_2O_2 was from Merck (Darmstadt, Germany). Reagents for electrophoresis were from Bio-Rad laboratories (Richmond, CA, USA) and other reagents were from Panreac (Barcelona, Spain). All reagents were of the highest purity available. Double-distilled water was used throughout. Unless otherwise indicated, experiments were carried out in 10 mM Na–phosphate buffer, pH 3.0.

The crude aPrx was isolated from the spent medium of peanut cell suspension culture [10]. Then aPrx was purified as described elsewhere [14]. For this, 3 g of the crude aPrx were dissolved in 50 ml of 0.1 M phosphate buffer, pH 6.5 and applied to a Phenyl-Sepharose column (1.5 cm × 25 cm) equilibrated with 0.1 M phosphate buffer pH 6.5, containing 1.4 M $(NH_4)_2SO_4$. The enzyme was eluted by 0.1 M phosphate buffer pH 6.5, containing 1.2 M $(NH_4)_2SO_4$ at a flow rate of 32 ml h^{-1}. The fractions having the peroxidase activity were collected and applied on a Sephacryl S 200 column (2.5 cm × 58 cm) equilibrated with 5 mM Tris pH 8.2 at a flow rate of 50 ml h^{-1}. The aPrx solution obtained at the gel-filtration was applied to a DEAE-Toyopearl column (0.9 cm × 9 cm) equilibrated with 5 mM Tris pH 8.2. Finally, the peroxidase was eluted with a linear (0–100 mM) NaCl gradient at a flow rate of 30 ml h^{-1}. The fractions containing peroxidase activity were collected, dialysed against distilled water, freeze–dried and stored at 5 °C.

The purity and molecular mass of the peroxidase were determined by SDS-PAGE. Electrophoresis was performed as described by Fairbanks et al. [15] on a Bio-Rad minigel apparatus using a flat block with a polyacrylamide gradient of 5–25%. Gels were prefixed and stained using the method of Merril et al. [16]. Analytical isoelectrofocusing was performed using Ampholine PAGE plates (Amersham-Pharmacia) with a pH range of 3–10. Electrophoretic conditions and silver staining were carried out as recommended by the manufacturer. The standards used were broad pI calibration kit (pH 3–10) from Amersham-Pharmacia. The protein contents were determined by the Bradford assay [17]. The RZ (ratio of A_{403}/A_{280}) for the aPrx samples used in this work was 2.5.

Peroxidase activity toward guaiacol was measured spectrophotometrically using a Hitachi U2000 spectrophotometer at 25 °C. An aliquot of enzyme solution was added to a spectral cuvette with 1 cm optical path length containing 18 mM guaiacol and 4 mM H_2O_2 in 20 mM potassium phosphate buffer, pH 7.0 in a final volume of 1 ml. The rate of change in absorbance due to substrate oxidation was monitored at 470 nm. Activities were calculated using a molar absorption coefficient of the guaiacol oxidation product at 470 nm of 5200 M^{-1} cm^{-1} [18].

The calorimetric experiments were performed on a MicroCal MC-2D differential scanning microcalorimeter (MicroCal Inc., Northampton, MA) with cell volumes of 1.22 ml, interfaced with a personal computer (IBM-compatible) as described previously [19]. Different scan rates within the 0.5–1.5 K min^{-1} range were employed. Before measurement, sample and reference solutions were properly degassed in an evacuated chamber for 5 min at room temperature and carefully loaded into the cells to avoid bubble formation. Exhaustive cleaning of the cells was undertaken before each experiment. An overpressure of 2 atm of dry nitrogen was always kept over the liquids in the cells throughout the scans to prevent any degassing during heating. A background scan collected with a buffer in both cells was subtracted from each scan. The reversibility of the thermal transitions was checked by examining the reproducibility of the calorimetric trace in a second heating of the sample immediately after cooling from the first scan. The experimental calorimetric traces were corrected for the effect of instrument response time using the procedure described previously [20]. The excess heat capacity functions

were plotted after normalisation ($M = 41{,}000\,\mathrm{g\,mol^{-1}}$) and chemical baseline subtraction using the Windows-based software package (Origin) supplied by MicroCal. Data were analysed by the non-linear least-squares fitting programs, as reported elsewhere [21].

Steady state fluorescence measurements were performed on a Hitachi F-4010 spectrofluorimeter. Excitation was at 280 nm (with excitation and emission slit widths of 5 nm). The fluorescence measurements of aPrx were carried out on protein solutions with an optical density of less than 0.2 at 280 nm to avoid the inner filter effect. All emission spectra were corrected for instrumental spectral sensitivity and fitted to the model of discrete states of tryptophan residues in proteins [22]. The temperature dependence of the characteristics of the fluorescence spectra were investigated using thermostatically-controlled water circulating in a hollow brass cell-holder. Temperature in the sample cell was monitored with a thermocouple immersed in the cell under observation. The heating rate was ca. $1\,\mathrm{K\,min^{-1}}$, and spectra were collected at desired temperatures over the entire temperature range. In titration experiments, pH values were adjusted by means of polyethylene rod moistened with either 0.1 M HCl or 0.1 M NaOH.

The far-UV CD spectra (190–250 nm) of aPrx were recorded on a Jasco-715 spectropolarimeter, using a spectral band pass of 2 nm and a cell path length of 1 mM with a protein concentration of ca. $0.2\,\mathrm{mg\,ml^{-1}}$. Spectra are averages of four scans at a scan rate of $20\,\mathrm{nm\,min^{-1}}$. All spectra were background-corrected, smoothed, and converted to mean residue ellipticity $[\Theta] = 10 M_{\mathrm{res}} \Theta_{\mathrm{obs}} l^{-1} p^{-1}$, where $M_{\mathrm{res}} = 115.5$ is the mean residue molar mass, Θ_{obs} is the ellipticity measured (°) at wavelength λ, l is the optical path length of the cell (dm), and p is the protein concentration ($\mathrm{mg\,ml^{-1}}$). Spectra were analysed using the SELCON3 software package [23]. To study the dependence of ellipticity on temperature, the samples were heated at a constant heating rate (ca. $1\,\mathrm{K\,min^{-1}}$) using a Neslab RT-11 programmable water bath.

3. Results and discussion

It is known that the structural stability of peroxidases strongly depends on the pH of the solution [24–26]. Taking this into account we used the changes in the parameters of the intrinsic fluorescence spectra and CD, which carry information about the tertiary and secondary structure of the protein, accordingly, for determination of the pH-stability limit of aPrx. Fig. 1 shows the pH-dependence of the denatured fraction degree of aPrx measured by following the changes in fluorescence quantum yield and ellipticity at 210 nm since at this wavelength the changes in ellipticity are significant upon pH changes. It can be seen that, as in the case of HRP [25], only two conformational states arise in the course of pH decrease: a first one, which is the native state between pH 5 and 3, and a second conformational state that can be

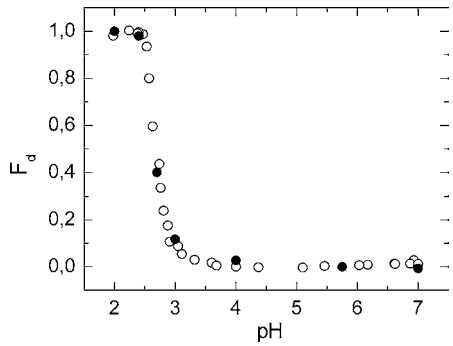

Fig. 1. Fractional degree of denaturation of aPrx as a function of pH monitored by the changes of fluorescence quantum yield (open symbols) and ellipticity at 222 nm (closed symbols) in 10 mM phosphate buffer at 293 K. Fraction of denatured aPrx, F_{d}, was calculated from the spectral parameters used to follow denaturation (y) prior to the minimization procedure, according to the expression: $F_{\mathrm{d}} = (y - y_n)/(y_{\mathrm{d}} - y_n)$, where $y_n = a_1 + a_2 x$ and $y_{\mathrm{d}} = b_1 + b_2 x$ represents the mean values of the y characteristic, obtained by linear regressions of pre- and post-transitional baselines; x is the variable parameter (pH in this case).

identified below pH 2.5, indicating that the acid denaturation of aPrx seems to be caused by titration of some carboxyl groups of enzyme amino acids. The data thus obtained served us as a basis for choosing a pH value of 3.0 to study the thermal stability of aPrx in an attempt to compare the stability of this enzyme with other ones studied at the same conditions [19,25].

The thermal denaturation of aPrx at pH 3.0 gave rise to a well defined DSC transition, whose apparent T_{m} (temperature at the maximum of the heat capacity profile) depended on the scan rate. This effect can be seen in Fig. 2, where the thermal transitions for aPrx at three scan rates is shown. The thermal denaturation of aPrx was always calorimetrically irreversible since in a second heating of the enzyme solution no thermal effect was observed. Inspection of the DSC transitions shown in Fig. 2 further reveals asymmetry in the shape of the curves, which might arise from two

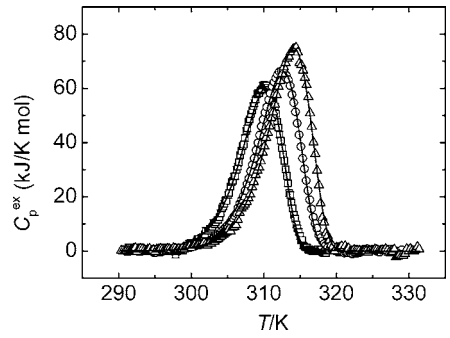

Fig. 2. Temperature dependence of the excess molar heat capacity of aPrx at scan rates of 0.5 (squares), 1.0 (circles) and 1.5 $\mathrm{K\,min^{-1}}$ (triangles) at pH 3.0. Solid lines are the best fit to each experimental curve using Eq. (2). Protein concentration were ca. $1.8\,\mathrm{mg\,ml^{-1}}$ at a scan rate of $0.5\,\mathrm{K\,min^{-1}}$, ca. $1.1\,\mathrm{mg\,ml^{-1}}$ at a scan rates of $1.0\,\mathrm{K\,min^{-1}}$, and ca. $0.8\,\mathrm{mg\,ml^{-1}}$ at a scan rate of $1.5\,\mathrm{K\,min^{-1}}$.

overlapping transitions. This would be a reasonable possibility for aPrx, which is a fairly large protein and may, in principle, comprise several domains [27]. We analysed this possibility by applying the successive annealing procedure [28]. Thus, aPrx was first heated at a scan rate 60 K h^{-1} in the microcalorimeter cell to a temperature 310 K, which would be close to the maximum for a putative first transition. Then the sample was cooled and heated again to 330 K at the same scan rate as before. The reheating scan revealed that the only effect of the first scan was to decrease the peak intensity by a scale factor determined by the difference in the amounts of protein undergoing irreversible denaturation, and that there was no change in T_m or any effect on the shape of the curve (not shown). This experiment rules out the possibility of overlapping independent transitions. The effect of the scan rate on the calorimetric profiles (T_m is shifted towards higher temperatures as scanning rate increases) clearly indicated that they corresponded to irreversible, kinetically controlled transitions and thus it is evident that equilibrium thermodynamics cannot be applied in their analysis [29,30]. Analysis of the DSC transitions was therefore accomplished on the basis of a simple two-state irreversible model (1). It should be noted here that in most cases irreversible thermal denaturation of proteins was sufficiently described by this simplest model alone [31], in which only the native (N) and final (irreversibly denatured) (D) states are significantly populated and the conversion from N to D is determined by a strongly temperature-dependent, first-order rate constant (k) that changes with temperature, as given by the Arrhenius equation: $k = \exp\{E_A(1/T^* - 1/T)/R\}$, where E_A is the energy of activation, R is the gas constant, and T^* is the temperature at which the rate constant equals 1 min^{-1}. In this case, the excess heat capacity C_p^{ex} is given by the following equation [21]:

$$C_p^{ex} = \frac{1}{\nu}\Delta H \exp\left\{\frac{E_A}{R}\left(\frac{1}{T^*} - \frac{1}{T}\right)\right\} \times \exp\left\{-\frac{1}{\nu}\int_{T_0}^{T} \exp\left[\frac{E_A}{R}\left(\frac{1}{T^*} - \frac{1}{T}\right)\right] dT\right\} \quad (2)$$

where $\nu = dT/dt$ (K min^{-1}) is the scan rate, ΔH is the enthalpy difference between the denatured and native states.

The excess heat capacity functions obtained for aPrx were analysed by fitting the data to the two-state irreversible model (Eq. (2)), either individually or globally, using scan rate as an additional variable. The results of fitting are shown in Fig. 2 (solid lines) and in Table 1. As can be seen, when fitting was carried out either separately on the individual experimental curves or simultaneously on all the curves, a good approximation was achieved. It is evident that the approximation is not very precise, probably due to differences in the values of the enthalpy of the denaturation process obtained at different scanning rates. At present, the reason for this difference remains unclear, although it could be related to a process of aggregate formation, which may accompany protein denaturation [32], and whose form depends on the rate of denaturation [33]. Attempts to include different irreversible models for aPrx denaturation—the Lumry–Eyring model, with a fast equilibrating first step, and the model that includes two consecutive irreversible steps [34,35]—did not improve the goodness of the fit, indicating that the two-state irreversible model is sufficient to describe aPrx denaturation quantitatively. This conclusion was further confirmed by our spectral and enzymatic activity investigations of the thermal denaturation of this enzyme. It should be noted additionally that no dependence of any of the parameters of DSC transitions on the aPrx concentration was found in the 0.5–2.4 mg ml^{-1} range.

Environmental changes in aromatic side chains resulting from conformational changes in the tertiary structure of proteins can be measured by intrinsic fluorescence spectroscopy. Fig. 3 shows the fluorescence spectra of intact (a) and thermally denatured, (b) aPrx at pH 3.0, excited at 280 nm. The fluorescence emission of the intact aPrx has a very low quantum yield (Fig. 3a) due to energy transfer to heme which, as can be seen in Fig. 3b, essentially increases in the denatured enzyme owing to a change in the relative orientation or distance between the heme and the tryptophan residue(s) [36]. Analysis of the spectra in terms of the model of discrete states of tryptophan residues in proteins [22] shows that the tryptophan residues of the I (emission of the indole chromophore located inside the protein globule and forming a 2:1 exiplex with some neighbouring polar protein group) and II (emission of the chromophore which is in contact with bound water) forms provide the main contributions to

Table 1
Arrhenius equation parameter estimates for the two-state irreversible model of the thermal denaturation of aPrx at pH 3.0[a]

Parameter	Temperature scan rate (K min^{-1})			
	0.5	1.0	1.5	Global fitting
ΔH (kJ mol^{-1})	448 ± 8	502 ± 6	573 ± 6	
T^* (K)	315.1 ± 0.2	315.6 ± 0.1	316 ± 0.1	315.9 ± 0.2
E_A (kJ mol^{-1})	287.4 ± 2.8	285.3 ± 2.6	285.3 ± 2.4	274.9 ± 3.6
r	0.9986	0.9989	0.9993	0.9948

[a] The correlation coefficient (r) which used as criterion for accuracy of fitting was calculated as $r = \sqrt{1 - \sum_{i=1}^{n}(y_i - y_i^{calc})^2 / \sum_{i=1}^{n}(y_i - y_i^{m})^2}$, where y_i and y_i^{calc} are respectively the experimental and calculated values of C_p^{ex}; y_i^{m} is the mean of the experimental values of C_p^{ex} and n is the number of points.

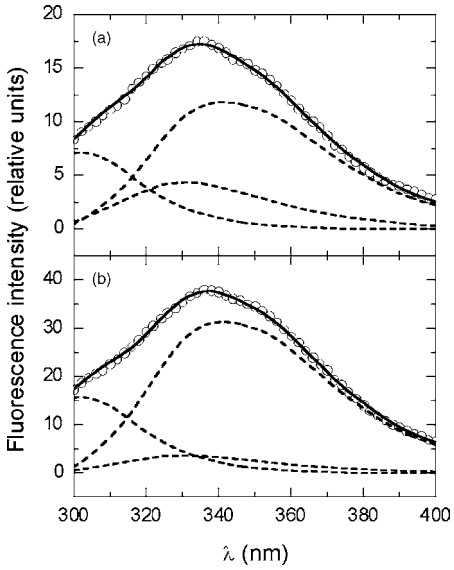

Fig. 3. Fitting of the experimental fluorescence spectra of intact at 293 K (a) and thermally-denatured at 325 K (b) aPrx (symbols) at pH 3.0 to the theoretical model of discrete states of tryptophan residues in proteins [22] (solid lines), which are the sums of the spectral components in order from left to right: tyrosine, I and II (dashed lines).

the tryptophan residues emission. The difference is only in quantity of these contributions: 25% of form I and 75% of form II for native aPrx and 10% of form I and 90% of form II for denatured one. From these data and the data offered below it is possible to conclude that a considerable portion of the secondary and tertiary structure elements persists in the thermally denatured state of aPrx.

In view of results presented above, we used the changes in fluorescence intensity to analyse the effect of temperature on process of aPrx denaturation. On increasing temperature (Fig. 4, solid symbols), irreversible co-operative transition to the denatured state occurred, which was analysed with non-linear least squares fitting to the equation:

$$F_d = 1 - \exp\left\{-\frac{1}{\nu}\int_{T_0}^{T} \exp\left[\frac{E_A}{R}\left(\frac{1}{T^*} - \frac{1}{T}\right)\right] dT\right\} \quad (3)$$

which is valid for model (1) and where F_d refers to the denatured fraction [21]. This fitting (solid line in Fig. 4) afforded the T^* parameter and the activation energy for aPrx. These results were 315.7 ± 1.2 K and 284.5 ± 3.2 kJ mol^{-1}, respectively, which are in satisfactory agreement with the values obtained from DSC experiments (Table 1).

The same experimental approach was applied to the enzymatic activity assays, as the denaturation of any enzyme is expected to abolish its biological activity, allowing us to monitor thermally induced conformational changes in the catalytic surrounding by measuring the loss of activity versus temperature while heating at constant rate (Fig. 4, open symbols). The value of the activation energy (286.2 ± 2.8 kJ mol^{-1}) and T^* (315.0 ± 1.1 K) obtained by fitting of experimental data to Eq. (3) are practically the same as obtained from fluorescence experiments.

The CD spectra of intact and thermally denatured aPrx at pH 3.0 are shown in Fig. 5. The spectrum in the intact state is characterised by double minima at 208 and 222 nm, respectively, which are indicative of an α–helical structure. The fractions of α-helix, β-strand, β-turn and unordered secondary structures obtained following the SELCON3 self-consistent method [23] are given in Table 2. It is interesting to note that the values thus obtained for intact aPrx are in reasonable agreement with the spatial structure of cPrx, which shows the presence of 46.9% of α-helices and only 2% of β-strands [9] and that content of secondary structure elements for both isozymes are typical for different heme peroxidases [37].

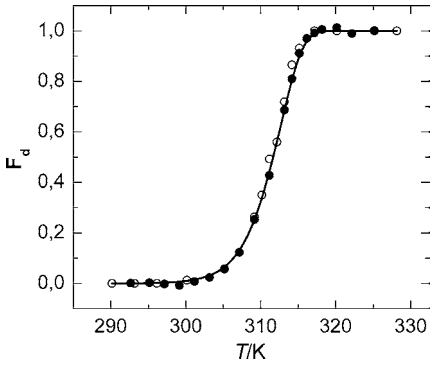

Fig. 4. Fractional degree of denaturation of aPrx as a function of temperature monitored by the changes of fluorescence quantum yield (open symbols) and enzymatic activity upon heating with a constant scan rate ca. 1 K min^{-1}. Solid line is the result of fitting the experimental data to the two-state irreversible denaturation model using Eq. (3). The experiments were performed in 10 mM phosphate buffer at pH 3.0. For other details see legend to Fig. 1.

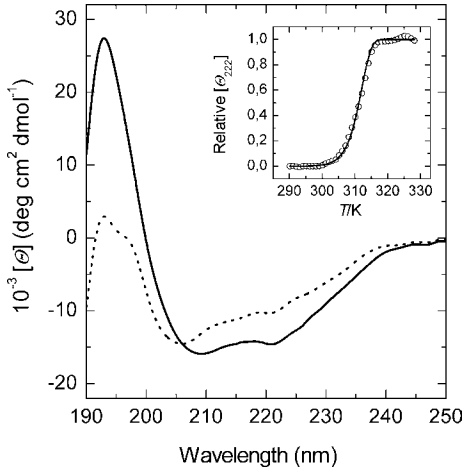

Fig. 5. Far-UV CD spectra of intact (solid lines) at 293 K and thermally denatured (dashed lines) at 325 K aPrx at pH 3.0. Inset: fractional degree of denaturation of aPrx as a function of temperature monitored by the changes of ellipticity at 222 nm in 10 mM phosphate buffer at pH 3.0 upon heating with a constant scan rate ca. 1 K min^{-1}. Solid line is the result of fitting the experimental data to the two-state irreversible denaturation model using Eq. (3). For other details, see legend to Fig. 1.

Table 2
Secondary structure elements (%) determined by CD spectroscopy for intact and thermally denatured aPrx at pH 3.0

Protein	α-Helix			β-Strand			β-Turn	Unordered
	Regular	Distorted	Total	Regular	Distorted	Total		
Intact	25.8	21.4	47.2	2.5	3.7	6.2	26.6	20.0
Denatured	15.1	15.3	30.4	4.0	5.0	9.0	23.2	37.4

Upon heating the aPrx to the denaturation temperature, the shape of the spectrum changes, showing an increase in unordered structure at the expense mainly of the α-helical structure (see Table 2). The increase in the quantity of β-strands that also takes place in denatured aPrx indicates that this form of the enzyme undergoes some aggregation, most probably of intramolecular character, because we failed to detect an increase in turbidity in the denaturation process.

The thermal denaturation of aPrx was monitored by following the changes in molar ellipticity at 222 nm since at this wavelength the changes in ellipticity are significant upon enzyme denaturation. On increasing temperature (Fig. 5, insert), irreversible co-operative transitions to the denatured state occurred, which were analysed using a non-linear least squares fitting to Eq. (3) (see line through the data points). This fitting affords the T^* parameter and the activation energy for aPrx. These results are 315.1 ± 2.7 K and 287.4 ± 4.2 kJ mol^{-1}, respectively, which are similar to the values for the same parameters obtained by the other methods used in this work. Thus, all these independent experimental approaches support the conclusion that aPrx thermal denaturation can be interpreted in terms of the irreversible two-state kinetic model, and that only two states, native and denatured are populated in its denaturation process.

Finally, we note that comparison data obtained in this work with data that we reported in our previous publications [19,25] permit us to conclude that aPrx is less thermostable than other peroxidases studied under the same experimental conditions. Thus, the T_m for aPrx at a scan rate of 1 K min^{-1} is 312.5 ± 0.2 K while for HRP*c* this value is 333.3 ± 0.2 K and for peroxidase from leaves of the African oil palm tree *Elaeis guineensis* (AOPTP) this value is 345.4 ± 0.2 K. The same situation takes place for T^*. Thus, T^* for aPrx is 315.4 ± 0.4 K while for HRP*c* this value is 342.7 ± 0.6 K and for AOPTP it is 347.2 ± 0.6 K. The higher value of energy of activation for aPrx (284.0 ± 2.4 kJ mol^{-1}) in comparison with the same value for HRP*c* (159.9 ± 2.1 kJ mol^{-1}) shows a higher degree of co-operativity in aPrx denaturation.

Acknowledgements

This work was supported by NATO Linkage Grant LST.CLG 978865 to M.G.R., I.Y.S., R.B.H. and V.L.S. D.G.P. is a fellowship holder from Fundação para a Ciência e a Tecnologia, Portugal (Ref. SFRH/BD/1067/2000).

References

[1] H.B. Dunford Heme Peroxidases, Wiley-VCH, New York, Chichester, Winheim, Brisbane, Singapore, Toronto.
[2] K.G. Welinder, Curr. Opin. Struct. Biol. 2 (1992) 388.
[3] A.T. Smith, N.C. Veitch, Curr. Opin. Chem. Biol. 2 (1998) 269.
[4] N.C. Veitch, A.T. Smith, Adv. Inorg. Chem. 51 (2001) 107.
[5] S. Colonna, N. Gaggero, C. Richelmi, P. Pasta, TIBTECH 17 (1999) 163.
[6] A.M. Egorov, E.M. Gavrilova, I.Yu. Sakharov, in: H. Greppin, C. Penel, W.J. Broughton, R. Strasser (Eds.), Integrated Plant Systems, University of Geneva, 2000, p. 369.
[7] W. Liu, A.L. Cholli, R. Nagarajan, J. Kumar, S. Tripathy, F.F. Bruno, L. Samuelson, J. Am. Chem. Soc. 121 (1999) 71.
[8] R.B. van Huystee, Y. Sun, B. Lige, Crit. Rev. Biotechnol. 22 (2002) 335.
[9] D.J. Schuller, N. Ban, R.B. van Huystee, A. McPherson, T. Poulos, Structure 4 (1996) 311.
[10] R.N. Chibbar, R.B. van Huystee, Plant Physiol. 75 (1984) 294.
[11] D. Stephan, R.B. van Huystee, Pflanzen Physiol. 101 (1981) 313.
[12] C.F. Hu, R.B. van Huystee, Biochem. Biophys. Res. Commun. 163 (1989) 689.
[13] R. Lumry, E. Eyring, J. Phys. Chem. 58 (1954) 110.
[14] I.Yu. Sakharov, J. Castillo, J.C. Ariza, I.Yu. Galaev, Bioseparation 9 (2000) 125.
[15] G. Fairbanks, T.L. Steck, D.F.N. Wallach, Biochemistry 10 (1971) 2606.
[16] C.R. Merril, D. Goldman, S.A. Sedman, M.H. Ebert, Science 211 (1981) 1437.
[17] M.M. Bradford, Anal. Biochem. 72 (1976) 248.
[18] A. Lindgren, T. Ruzgas, L. Gorton, E. Csöregi, G.B. Ardila, I.Yu. Sakharov, I.G. Gazaryan, Biosens. Bioelectron. 15 (2000) 491.
[19] A. Rodríguez, D.G. Pina, B. Yélamos, J.J. Castillo Leon, G.G. Zhadan, E. Villar, F. Gavilanes, M.G. Roig, I.Yu. Sakharov, V.L. Shnyrov, Eur. J. Biochem. 269 (2002) 2584.
[20] O. Lopez Mayorga, E. Freire, Biophys. Chem. 87 (1987) 87.
[21] B.I. Kurganov, A.E. Lyubarev, J.M. Sanchez-Ruiz, V.L. Shnyrov, Biophys. Chem. 69 (1997) 125.
[22] Y.K. Reshetnyak, E.A. Burstein, Biophys. J. 81 (2001) 1710.
[23] N. Sreerama, S.Yu. Venyaminov, R.W. Woody, Prot. Sci. 8 (1999) 370.
[24] J.W. Tams, K.G. Welinder, Biochemistry 35 (1996) 7573.
[25] D.G. Pina, A.V. Shnyrova, F. Gavilanes, A. Rodríguez, F. Leal, M.G. Roig, I.Yu. Sakharov, G.G. Zhadan, E. Villar, V.L. Shnyrov, Eur. J. Biochem. 268 (2001) 120.
[26] I.Yu. Sakharov, I.V. Sakharova, Biochim. Biophys. Acta 1598 (2002) 108.
[27] J.R. Garel, in: T.E. Creighton (Ed.), Protein Folding, Freeman, New York, 1992, p. 405.
[28] V.L. Shnyrov, G.G. Zhadan, in: S.G. Pandalai (Ed.) Recent Research and Development in Physical Chemistry, Transworld Research Network, Trivandrum, India, 2000, p. 351.

[29] E. Freire, W.W. van Osdol, O.L. Mayorga, J.M. Sanchez-Ruiz, Annu. Rev. Biophys. Biophys. Chem. 19 (1990) 159.
[30] J.M. Sanchez-Ruiz, Biophys. J. 61 (1992) 921.
[31] I.M. Plaza del Pino, B. Ibarra-Molero, J.M. Sanchez-Ruiz, Proteins 40 (2000) 58.
[32] M. Joly, A Physico-chemical Approach to the Denaturation of Proteins, Academic Press, New York, 1965.
[33] B.I. Kurganov, Biochemistry (Moscow) 63 (1998) 430.
[34] A.E. Lyubarev, B.I. Kurganov, Biochemistry (Moscow) 63 (1998) 434.
[35] A.E. Lyubarev, B.I. Kurganov, Biochemistry (Moscow) 64 (1999) 832.
[36] B.C. Hill, P.M. Horowitz, N.C. Robinson, Biochemistry 25 (1986) 2287.
[37] L. Banci, J. Biotechnol. 53 (1997) 253.